Order-disorder transformation in Au-Cu alloys studied by extended x-ray-absorption fine structure

T. Claeson
Physics Department, Chalmers University of Technology, S-412 96 Gothenburg, Sweden

J. B. Boyce
Xerox Palo Alto Research Center, Palo Alto, California 94304
(Received 12 August 1983)

We show that extended x-ray-absorption fine-structure studies can estimate the degree of short-range order both above and below the transformation temperature of alloys displaying superlattices at low temperature. A substantial degree of short-range order was measured above the ordering temperature of 390 °C for $AuCu_3$. The local Au-Cu pair separation and its fluctuation show discontinuities at the ordering temperature. Shifts in the absorption edge were also observed at the transformation.

INTRODUCTION

Several alloy systems display a structural order-disorder transformation.[1] Well above the ordering temperature T_0, the constituent A and B atoms randomly occupy the lattice sites, while below T_0 a superlattice is formed at stoichiometric compositions with A and B on interpenetrating lattice positions. The Au-Cu system is a classical example of alloys with superlattice formation. Au_3Cu orders[2] at $T_0=200$ °C, AuCu at 408 °C, and $AuCu_3$ at 390 °C. The cubic lattice is retained in the ordered Au_3Cu and $AuCu_3$ alloys but is slightly distorted tetragonally in AuCu.

Although the transformation at T_0 is distinct with discontinuities in many physical parameters, the order (disorder) below (above) T_0 is not complete even at the stoichiometric alloy composition. Below T_0 the long-range-order parameter S approaches 1 at $T=0$; it becomes somewhat less than 1 at $T\rightarrow T_0$. Above T_0 the long-range order is zero. However, there exists a temperature-dependent short-range order, a preference of A atoms to be surrounded by B atoms, and a preference of B atoms to be surrounded by A atoms. X-ray techniques have been employed to study the degree of order: The intensities of the superlattice diffraction lines give the long-range-order parameter, S, while diffuse x-ray scattering, with maximum intensities at the former superlattice reflections, gives short-range-order coefficients related to the short-range-order parameter σ_{SRO}. These measurements of the short-range order are tedious and several corrections have to be made in the extraction procedure.

Extended x-ray-absorption fine structure (EXAFS) is a method well suited for the determination of the local order around absorbing atoms. The absorption of x-ray photons results in the emission of electrons from inner shells. These electrons may be scattered by neighbor atoms before being recaptured. The interference between the outgoing and backscattered electron waves results in fine structure at photon energies just above the absorption threshold. An analysis of the EXAFS can give the numbers of the different neighbors around the absorbers, their separations, and the spreads in the neighbor distances.

In this work, we use EXAFS to determine the probabilities of finding A and B neighbors to an atom A, as well as the corresponding separations at temperatures around the ordering temperature of the A-B alloys. Our analysis effort was concentrated on the $AuCu_3$ alloy, which is well suited for this type of study.

EXPERIMENTS

Au (Johnson, Matthey, and Company, Ltd., 99.99% purity) and Cu (Johnson, Matthey, and Company, Ltd., 99.999% purity), in proportions to give alloys of compositions 24.9, 49.9, and 75.0 at. % Cu, were encapsulated in quartz tubes under helium atmospheres and melted for 15 min in an rf furnace (1100 °C). Pieces of the slowly cooled ingots were heat-treated at 700 °C for 2 h and slowly cooled to about 350 °C, where they were kept for a day. The sheets were later rerolled to a thickness of about 10 μm giving an x-ray transmission of about 8% at the Au and Cu absorption edges. That rerolling was followed by anneals at 800 °C for 80 min, 550 °C for 100 min, 359 °C for 46 h, 163 °C for 10 h (Au_3Cu, 21 h), and room temperature for 90 h.

Incident- and transmitted-radiation intensities were registered by ionization (N_2-gas) counters at energies around the Cu K (8.98 keV) and Au L_{III} (11.92 keV) absorption edges. The experiments were performed at one of the wiggler lines (VII-2) of the Stanford Synchrotron Radiation Laboratory under dedicated operating conditions at 3 GeV. A computer-controlled, stepped Si(220) crystal monochromator selected the radiation wavelengths. It was detuned to half maximum intensity in the rocking curve in order to suppress the harmonic content of the incident radiation. The energy resolution was approximately 1 eV.

Two sample mountings were utilized. In both, the sam-

ples were surrounded by an exchange gas of helium, either in a cryostat for measurements between room and liquid-nitrogen temperature, or, between boron nitride clamping plates, in a furnace for elevated temperatures. The temperature was measured with a thermocouple and controlled within a couple of degrees of the desired temperature. It is important to ascertain whether the samples were in thermodynamic equilibrium or not during the measurements. The ordering is a sluggish process with times to reach equilibrium increasing exponentially with inverse temperature.[1] The time available in a synchrotron-radiation experiment is by necessity limited and the anneal times must be short if we want to use the same sample at different temperatures. Preferably, we should have monitored the degree of order by measuring the resistance of the foil or the diffuse x-ray scattering during the experiment, but this was not done. However, the degree of order that is measured by different methods depends upon the type of experiment. For example, the resistance caused by small antiphase domains may mask the development of order. In our case we measure short-range-order properties, and the times needed to reach a sufficiently transformed state may be considerably shorter than in a resistance experiment.

We encounter at least three relaxation times[3] in reaching an equilibrium order in our experiment: $\tau_{d\to 0}$ is a measure of the exponential relaxation time to develop a long-range-ordered state from the disordered state in a sample cooled below T_0; $\tau_{0\to 0}$ is a measure of the relaxation time for changes in the already ordered state, either increasing the order further by cooling a previously annealed and ordered sample or decreasing the order by heating; $\tau_{0\to d}$, finally, determines the transformation of an ordered state to a disordered one when the anneal temperature is raised above T_0. All these characteristic times increase exponentially with inverse temperature. $\tau_{d\to 0}$ further displays a pronounced slowdown in the vicinity of T_0. $\tau_{0\to 0}$ is considerably shorter than $\tau_{d\to 0}$ at a given temperature.[3]

In our experiment, an ordered state should have been fully developed in $AuCu_3$ (and AuCu) since the anneal time at about 350 °C was much longer than the $\tau_{d\to 0}$ which is of the order of a couple of hundred minutes as estimated from resistance changes.[3] The samples were then slowly cooled to room temperature (with an arrest midway) where they were kept several days. Although a fully developed long-range-ordered state might not have been obtained, the local, short-range order should be sufficiently developed. Hence, we think the measurements at room temperature are representative of the ordered phase at that temperature. In the measurements at 77 K, however, the cool down from room temperature was rapid, of the order of a few minutes. Thus the long-range order of the sample probably did not increase substantially at 77 K compared to that at room temperature—only the thermal disorder decreased.

Going to temperatures above room temperature, it took about 15 min to reach thermal equilibrium in the oven after which the data collection started within a few minutes. EXAFS data above the Cu K edge were registered after about 5 min. (At 500 °C, the sample got an extra hour of annealing due to a reinjection of the beam.) Although $\tau_{0\to 0}$ is much shorter than the commonly quoted $\tau_{d\to 0}$, it is questionable whether equilibrium order was attained at 200 and 250 °C. The corresponding values of $\tau_{d\to 0}$, from resistance measurements, were considerably longer than our anneal times. Going to a disordered state above T_0, the relaxation time becomes less than 10 min for a temperature larger than 700 K. Thus our high-temperature points should be representative of the equilibrium state.

RESULTS AND ANALYSIS

An example of the x-ray absorption around the L_{III} edge for Au in the $AuCu_3$ sample is given in Fig. 1. The energy E was scanned from about 1000 eV below to 1600 eV above the edge. A sharp rise in the absorption at the edge is followed by smaller oscillations as the photon energy is increased. Let us first comment on the edge position before presenting the EXAFS results.

By comparing the absorption curves taken at several temperatures (see Fig. 2) on the same sample, we can obtain a picture of the change in the electronic structure

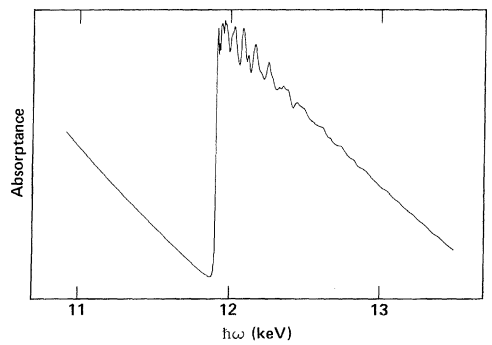

FIG. 1. X-ray absorption in the vicinity of the Au L_{III} edge of a 10-μm-thick $AuCu_3$ foil at 77 K.

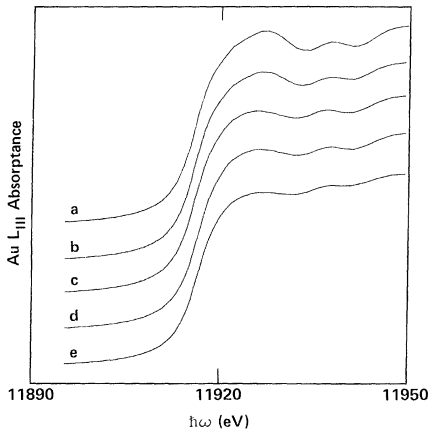

FIG. 2. Absorption at the Au L_{III} edge in $AuCu_3$ at several temperatures: a, 77 K and b, 623 K, both well below $T_0 \simeq 660$ K; c, 681 K in the vicinity of T_0; d, 774 K and e, 1198 K, both well above T_0.

caused by the order-disorder transformation. For $AuCu_3$, a change of about 0.5 eV in the absorption edge E_0 upon going from the low-temperature ordered phase to the high-temperature disordered phase was determined. E_0 was defined as the energy at one-half of the absorption rise at the edge. The locations of the first maxima and minima in the absorption above the edge are also shown in Fig. 3. As in E_0, they exhibit changes around the ordering temperature as shown for both the Au L_{III} and Cu K edges. Similar changes at the ordering temperature were noted for the AuCu sample but not for Au_3Cu.

A quantitative comparison between the absorption edges of the different samples is less accurate than the one of the same sample at several temperatures. The shape of the edge structures changes from alloy to alloy. In $AuCu_3$ and AuCu at 77 K, where the Au atoms have only Cu near neighbors, the difference between the Au L_{III} edges is small. The energies of the AuCu peaks are slightly smaller than those of $AuCu_3$, in accordance with Ref. 4, but the dissimilarities may well fall within the experimental uncertainty.

The analysis of the EXAFS above the absorption edges followed a standard procedure as outlined in Ref. 5. A slowly varying absorption background was subtracted, and the absorption cross section of the Au and Cu atoms above the edge (disregarding the fine structure) was approximated as a six-order polynomial in $(E-E_0)^{1/2}$. The data are then converted to $\vec{k}$ space ($\hbar^2k^2/2m=E-E_0$) where the EXAFS for a polycrystalline sample is given by

$$\chi(k)=\frac{1}{k}\sum_j \frac{N_jF_j(k)}{r_j^2}\sin[2kr_j+\delta_j(k)] \times e^{-2r_j/\lambda_e}e^{-2\sigma_j^2k^2}, \quad (1)$$

where the sum is taken over shells with N_j atoms at distance r_j from the absorber. σ_j^2 is the temperature-dependent mean-square fluctuation in r_j, $1/\lambda_e$ is a decay constant, i.e., the inverse mean free path for scattered electrons, and $F_j(k)$ and $\delta_j(k)$ are the backscattering amplitude and total phase shift which both depend upon the type of atom in shell j. The expression assumes that the pair correlation functions are Gaussians and does not account for any possible asymmetry in the peak shape. This is a good approximation at low temperatures but may not be appropriate at the highest temperatures. We assume, however, that any change in the peak shape from symmetric to antisymmetric is small compared with the changes due to an increase in σ_j and due to the disorder of the near-neighbor environment as the temperature is increased. Representative spectra in $\vec{k}$ space are shown in Fig. 4 for the EXAFS on the Au L_{III} edge at 77 K for Au, $AuCu_3$, AuCu, and Au_3Cu.

A comparison among different EXAFS data sets can be made in $\vec{k}$ space. However, the extraction of structural information is often facilitated in $\vec{r}$ space following a Fourier transform. In $\vec{r}$ space the peaks corresponding to

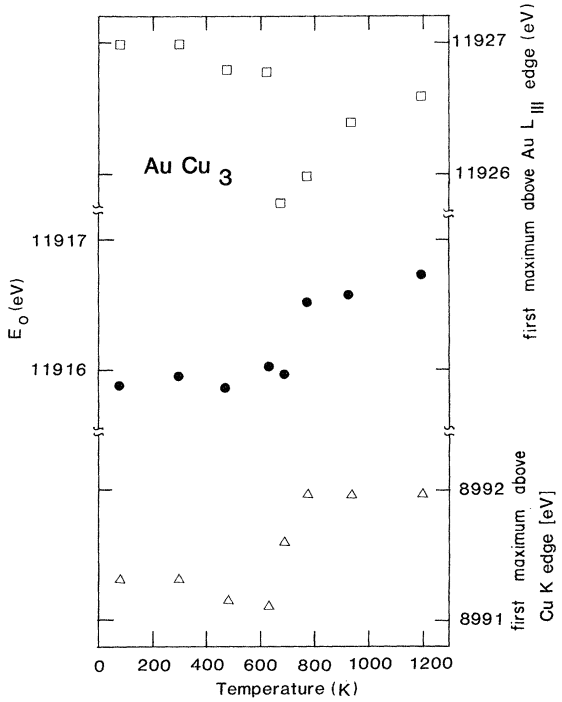

FIG. 3. Temperature dependence of absorption-edge features of $AuCu_3$. The circles denote the energies at the half value of the absorption rise at the Au L_{III} edge, and the squares denote the locations of the first maximum above the Au L_{III} edge for $AuCu_3$, which orders at about 660 K. The error bars for these points are approximately ±0.5 eV.

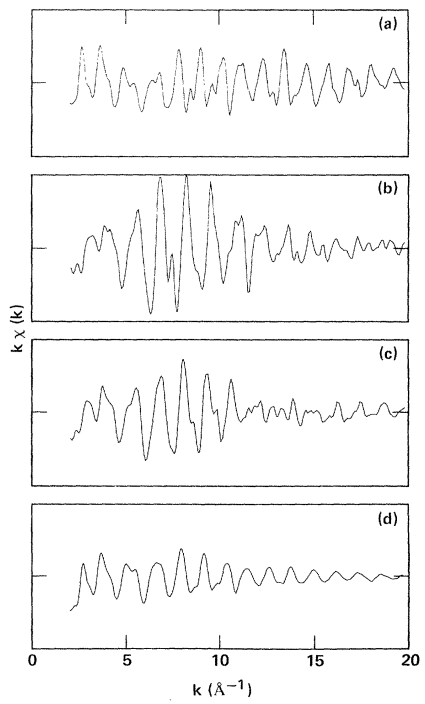

FIG. 4. EXAFS, $k\chi(k)$ vs k, on the Au L_{III} edge is 77 K for (a) Au, (b) $AuCu_3$, (c) AuCu, and (d) Au_3Cu. The vertical scale in each case is the same, varying from −0.55 to 0.55 Å^{-1}.

the various neighbors are often resolved from one another. This is shown in Fig. 5 for the Fourier transforms of the EXAFS on the Au L_{III} edge of the four spectra in Fig. 4. In each case the peaks between 2 and 3 Å represent the near-neighbor environment and are well resolved from the further-neighbor peaks. In the case of Au [Fig. 5(a)] this first peak corresponds to 12 Au atoms 2.88 Å and the double-peaked shape is due to structure in the backscattering amplitude $F(k)$ for the heavy Au backscatters. Contrast this with the $AuCu_3$ case [Fig. 5(b)] where the first-neighbor peak also corresponds to 12 near neighbors at a single distance but where the neighbors are Cu rather than Au. The differences are predominantly due to the differences in $F(k)$ for Au and Cu. The corresponding Cu-edge spectra at 77 K are shown in Fig. 6 for Cu metal and the three Au-Cu compounds.

Values of N_j, r_j, and σ_j can be obtained from the EXAFS data if the scattering amplitudes and phase shifts [cf. Eq. (1)] for the different backscatters are known. Theoretical values do exist,[6] but a more convenient and accurate method is to use separate standards for the Au-Au, Au-Cu, Cu-Au, and Cu-Cu neighbors (where the first element denotes the absorber and the second one the backscatterer). The foils of Au, $AuCu_3$, Au_3Cu, and Cu were used to give 77-K standard signatures and their spectra are shown in Figs. 4–6. At low temperature, the two alloys should be sufficiently well ordered, giving well-defined first neighbors to Au [i.e., Au-Cu pairs only; Fig. 5(b)] and to Cu [Cu-Au; Fig. 6(d)], respectively.

Our analysis concentrated on the $AuCu_3$ alloy, in which, for the ordered state, Au is surrounded by a first-neighbor Cu shell of 12 atoms at a single distance and the Cu has eight Cu neighbors and four Au neighbors at a single distance. The region around the first-neighbor peak in the Fourier transform of the Au L_{III} EXAFS at 77 K of that sample was used as a signature of the Au-Cu scattering [Fig. 5(b)]; the signature of pure Au at 77 K was used as the Au-Au signature [Fig. 5(a)]. The ordering temperature of $AuCu_3$ is relatively high, enabling disorder to develop during the short anneal time available in the experiment. In the Au_3Cu alloy, Cu has a well-defined Au first-neighbor environment in the ordered state. However, the transformation temperature is low and it is difficult to reach a state in reasonable equilibrium in that temperature range during a short time ($\sim$15 min). AuCu has an ordering temperature above that of Au_3Cu, but it deforms tetragonally, giving a spread of nearest-neighbor distances [see Figs. 5(c) and 6(c)]. As a result, these latter two alloys were not analyzed in much detail, and we concentrated on $AuCu_3$ instead.

The spectra for $AuCu_3$ at elevated temperatures are shown in Figs. 7–9. The temperatures chosen are (a) 208 °C well below $T_0 \simeq 390$ °C, (b) 408 °C in the vicinity of

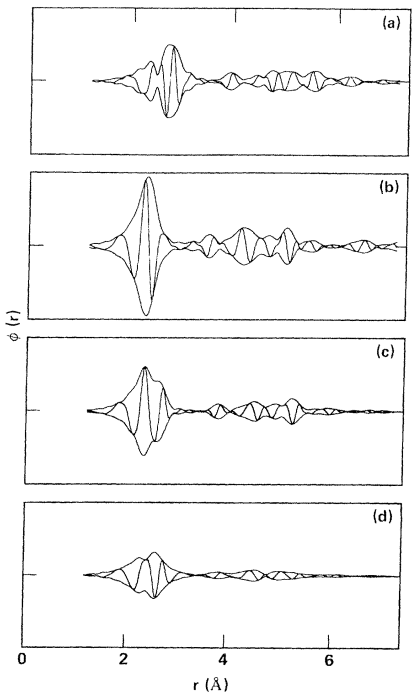

FIG. 5. Real part and magnitude (envelope) of the EXAFS in $\vec{r}$ space on the Au L_{III} edge at 77 K for (a) Au, (b) $AuCu_3$, (c) AuCu, and (d) Au_3Cu. These spectra are the Fourier transforms of the data in Fig. 4 using a square window from $k = 3.8$ to 18.9 Å^{-1} broadened by a Gaussian of width 0.7 Å^{-1}. In each case the vertical scale is the same, varying from -1.2 to 1.2 Å^{-2}.

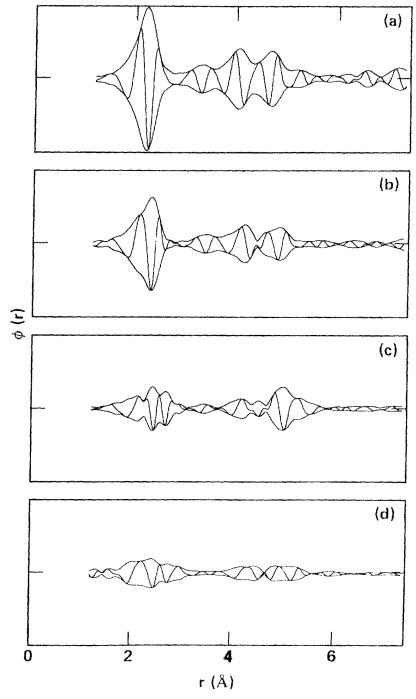

FIG. 6. Real part and magnitude (envelope) of the EXAFS in real space on the Cu K edge at 77 K for (a) Cu, (b) $AuCu_3$, (c) AuCu, and (d) Au_3Cu. The Fourier transforms were performed using a square window from $k = 3.6$ to 17.9 Å^{-1} broadened by a Gaussian of width 0.7 Å^{-1}. The vertical scales are the same, from -1.45 to 1.45 Å^{-2}.

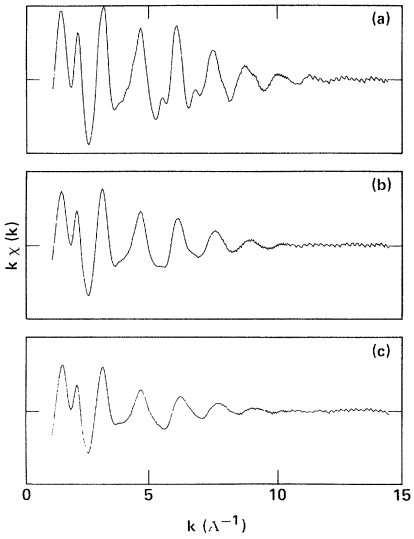

FIG. 7. EXAFS on the Cu K edge for $AuCu_3$ at three increasing temperatures: (a) 208 °C, well below $T_0 \simeq 390$ °C; (b) 408 °C, in the vicinity of T_0; and (c) 650 °C, well above T_0. The vertical scales are the same, from -0.28 to 0.28 Å^{-1}.

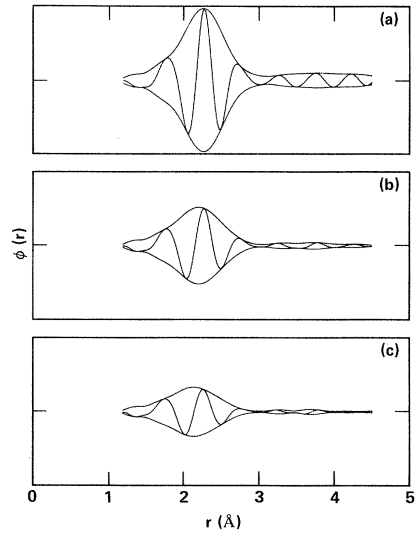

FIG. 9. Real part and the magnitude (envelope) of the EXAFS on the Au L_{III} edge of $AuCu_3$ in real space at (a) 208 °C, (b) 408 °C, and (c) 650 °C. The transform range is from $k = 3.9$ to 12.9 Å^{-1} broadened by a Gaussian of width 0.7 Å^{-1}. The vertical scales are the same, from -0.4 to 0.4 Å^{-2}.

T_0, and (c) 650 °C well above T_0. Figure 7 shows the EXAFS on the Cu K edge in $\vec{k}$ space at these temperatures. The increase in thermal damping is evident, yet an adequate signal-to-noise ratio is obtained at the highest temperature. The corresponding Fourier transforms of this Cu EXAFS are shown in Fig. 8, where it is seen that in addition to the broadening in the first-neighbor peak, the further-neighbor information decreases more rapidly with increasing temperature. As a result, we only analyzed the data on the first-neighbor peak, where significant information still remains at high temperatures. The corresponding EXAFS spectra on the Au L_{III} edge are shown in Fig. 9, where the same general trends are observed. Our analysis concentrated on this Au L_{III}—edge data to the simpler near-neighbor environment to the Au, i.e., only Cu near neighbors in the ordered state and nine Cu plus three Au neighbors in the totally disordered state.

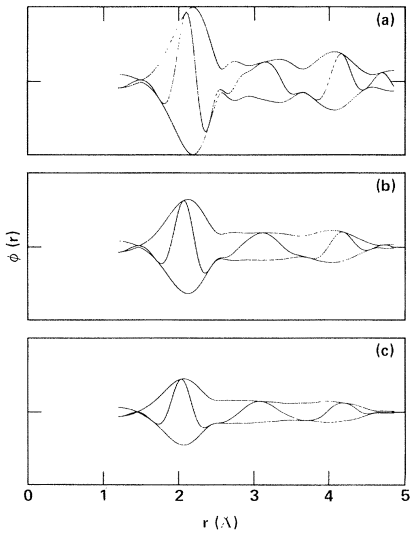

FIG. 8. Real part and magnitude (envelope) of the EXAFS on the Cu K edge of $AuCu_3$ transformed to real space at (a) 208 °C, (b) 408 °C, and (c) 650 °C. These are the Fourier transforms of the data of Fig. 7 using a square window from $k = 2.2$ to 12.3 Å^{-1} broadened by a Gaussian of width 0.7 Å^{-1}. The vertical scales are the same, from -0.36 to 0.36 Å^{-2}.

Restraints have to be introduced in the computer fits. Without such restraints, a six-parameter fit can easily find a false local minimum in the least-squares difference between the model and the measured complex Fourier transform $\Phi(r)$. The fit parameters used are $N_{Au\text{-}Au}$, $\Delta r_{Au\text{-}Au}$, $\Delta\sigma_{Au\text{-}Au}$, $N_{Au\text{-}Cu}$, $\Delta r_{Au\text{-}Cu}$, and $\Delta\sigma_{Au\text{-}Cu}$, where Δ denotes the difference between the sample and the 77-K standard. Well-behaved values were always obtained for the additional Debye-Waller—type broadenings of the pair radial distribution functions, so no restrictions had to be employed for the $\Delta\sigma_j$'s. Restraints on the distances to and the probabilities of finding Au or Cu neighbors had to be used. One obvious constraint is that the sum of the probabilities that a given neighbor to an Au atom in $AuCu_3$ is Au or Cu has to equal 1, i.e., $N_{Au\text{-}Au} + N_{Au\text{-}Cu} = 12$. An initial value of the neighbor separation was approximated using reported values of the lattice constant and its thermal expansion. Keeping this value fixed, the probabilities of Au and Cu first neighbors to an Au atom were obtained by optimizing the fit. These probabilities were then kept constant to give optimum values of the separation in a second set of fits. Finally, a number of fits with different fixed separation values (falling in a range around the previous optimum values) was made to obtain a best set of parameter values.

The temperature variations of the best set of values of $r_{\text{Au-Cu}}$, $(\Delta\sigma_{\text{Au-Cu}})^2$, and $A_{\text{Au-Au}}$, the probability of a first Au neighbor to an Au absorbing atom in $AuCu_3$, are given in Fig. 10. (This information was extracted from the Au L_{III} EXAFS.) Discontinuities at the ordering temperature are evident in the neighbor distances and in the widths of the near-neighbor distributions.

The probability of finding an Au-Au pair changes gradually from 0 to 0.25 as the transformation region is traversed. Similar tendencies as those in Fig. 10 were also noted for the other alloys, but due to the difficulties mentioned above, the uncertainties were much larger. The temperature variation of σ always showed a small discontinuity at the transformation temperature (although less pronounced in the Au_3Cu alloy). The number of Cu-Cu nearest neighbors in Au_3Cu increased gradually above the ordering temperature, but the reliability of these results is questionable due to uncertainties as to whether equilibrium had been reached. For the Cu EXAFS of the $AuCu_3$ sample, we could apply the probabilities of Cu-Au and Cu-Cu pairs obtained from the Au L_{III} EXAFS in the fits. This gave a similar $\sigma_{\text{Cu-Au}}$ behavior as in Fig. 10. However, the results using the Cu K-edge data are less reliable due to the more complex near-neighbor environment, i.e., both Cu and Au near neighbors.

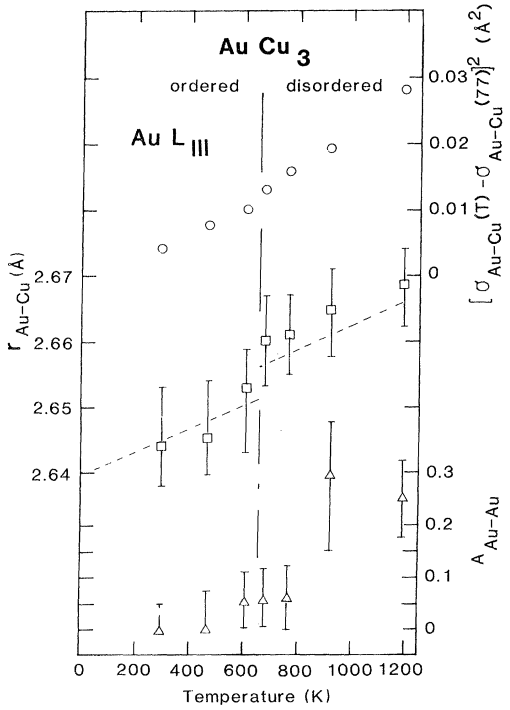

FIG. 10 Results for $AuCu_3$: The temperature dependence of $A_{\text{Au-Au}}$, the probability of finding an Au first neighbor to an Au absorber (triangles), of $r_{\text{Au-Cu}}$, the Au-Cu pair separation (squares), and of $\Delta\sigma^2_{\text{Au-Cu}}$, the mean-square fluctuation of that distance as compared to the 77-K value (circles). The parameters were obtained using Au L_{III} EXAFS of an $AuCu_3$ foil. The ordering temperature of the alloy is about 660 K.

DISCUSSION

From Fig. 10 we note that the probability of finding an Au atom in the first-neighbor shell of an Au absorber in $AuCu_3$ does not jump from 0 to the disordered value of $x_{\text{Au}}=0.25$ as the temperature traverses the ordering point. Instead, there seems to be an amount of disorder just below T_0 and likewise a considerable short-range order above T_0.

We can compare $A_{\text{Au-Cu}}$, our probability of finding an unlike atom in the first shell around Au in $AuCu_3$, with the short-range parameter α_1, introduced by Cowley,[7,8] or with Bethe's short-range-order parameter,[9] σ_{SRO}. For the first shell in $AuCu_3$, these are defined as:

$$\alpha_1^{\text{Au}}=1-A_{\text{Au-Cu}}/x_{\text{Cu}}=1-(\tfrac{4}{3})A_{\text{Au-Cu}}=-(\tfrac{1}{3})\sigma_{\text{SRO}}^{\text{Au}}\ .$$

Figure 11 compares the short-range-order parameters estimated from our EXAFS experiment with those determined from diffuse x-ray scattering.[7,10,11] The x-ray values determined by Moss[11] are the latest ones—the precautions taken in that work should lead to the most reliable values. The agreement between the different measurements is reasonable, particularly in view of the large uncertainties in the extraction of the parameters. Also shown is the theoretical curve computed[12,13] using an Ising model, and the Kikuchi approximation.[14]

As there is a preference of forming Au-Cu pairs, one would expect the Au-Cu separation to be smaller than the average lattice distance in the disordered state. Figure 10

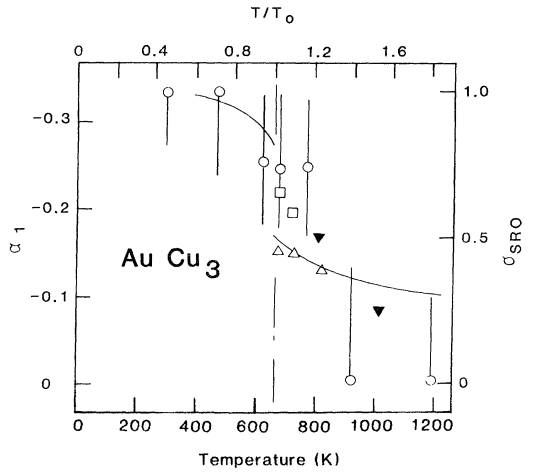

FIG. 11. Temperature dependence of two short-range-order parameters that give the probability of finding different nearest neighbors. Cowley's parameter α_1^{Au} and Bethe's $\sigma_{\text{SRO}}^{\text{Au}}$ measure the degree of deviation from the random value of the probability of finding a Cu neighbor next to a specified Au atom, x_{Cu}. They vanish for complete randomness and approach the values of $-\frac{1}{3}$ and 1, respectively, for completely ordered $AuCu_3$. The values extracted from the EXAFS analysis are given by the circles. They are compared with those from diffuse x-ray scattering; squares from Moss (Ref. 11), open triangles from Cowley (Ref. 7), and solid triangles from Wilchinsky (Ref. 10). The solid line is a theoretical result using an Ising model (Ref. 12).

does not justify this expectation. The thermal expansion is well duplicated,[15] but the average separation is somewhat larger than expected in the disordered state judging from the Au L_{III} EXAFS data. A word of caution should be given though. The uncertainty in the neighbor distance is considerable, and furthermore the Cu-Au pair separations extracted from the CuK −edge data for the same sample showed a decrease when it was heated above T_0.

The spread in the pair correlation function σ varies qualitatively as expected. When the long-range order is destroyed, there is a small discontinuous jump in σ to larger values, i.e., a larger spread of unlike neighbor distances. The slope of $[\Delta\sigma(T)]^2$ also changes. The ordered superlattice is stiffer than the disordered alloy. Its phonon frequencies are higher, and hence the thermal disorder is smaller. Several factors influence the change of the phonon spectrum at the order-disorder transformation: the discontinuous change in the average lattice constant, the mass disorder, the electronic screening due to changes in the electron structure, gaps in the phonon dispersion relation at Brillouin zones, and optical phonons occurring in a superlattice. The gradual decrease of the short-range order and the increase of the atomic separation with increasing temperature would tend to give a nonlinear temperature dependence of the pair correlation fluctuations. Figure 10, on the other hand, indicates linear dependences below and above T_0 (although small nonlinear contributions would disappear within the uncertainty in these parameters).

An Einstein model of the vibrational spectrum is the simplest, and often a useful, approximation in the calculation of the mean-square fluctuations in interatomic distances. The characteristic frequency ω_E of such an expression is a measure of the local vibrational structure of importance for the fluctuations in the correlated pair separation. An Einstein approximation gives roughly the same agreement with experimental $\sigma^2(T)$ as various force-constant models of the lattice vibrations do.[16] Such a treatment gives a linear temperature dependence of $\sigma^2 \approx 2kT/\overline{M}\omega_E$ at high temperature ($\overline{M}$ is the average mass). From the linear temperature dependences of Fig. 10, we infer a change of about 17% in the Einstein temperature at T_0 (from about 230 to 200 K). This large change can be compared with the 5—25 % change (in different symmetry directions) of the elastic constants[17] in an interval around the ordering temperature of $AuCu_3$. The latter measurements by Sieger[17] were made at relatively low frequencies.

Kuczynski *et al.*[18] reported a phase transition between 550 and 600 °C, and possibly another one near 850 °C, from measurements of the specific heat, the temperature coefficient of expansion, the Young's modulus, and the yield point of $AuCu_3$. No anomalies in these regions were evident from our EXAFS data.

CONCLUSION

We have shown that the degree of short-range order in a partially ordered alloy can be extracted from EXAFS data. The results agree on the whole with those of other measurements although our uncertainties are rather large. The interpretation of the EXAFS data is straightforward and it is possible to obtain values of the short-range-order parameter both above and below the ordering temperature. These values are difficult to obtain using other methods. The limited anneal times at low temperatures hampered the extraction of reliable parameter values below the ordering temperature for the AuCu and Au_3Cu samples in these first experiments. Owing to its higher T_0 value, the results on $AuCu_3$ well below the ordering temperature are representative of the ordered state.

In addition, the change in the absorption edge with temperature indicates that the superlattice formation may strongly influence the electronic structure of an alloy.

ACKNOWLEDGMENTS

Work done at the Stanford Synchrotron Radiation Laboratory was supported by the National Science Foundation through the Division of Materials Research and by the National Institutes of Health through the Biotechnology Resources Program in the Division of Research Resources (in cooperation with the U.S. Department of Energy). Support was also obtained from the Swedish Natural Science Research Council. Helpful discussions with J.C. Mikkelsen, Jr. are acknowledged.

[1]For reviews, see, e.g., T. Muto and Y. Takagi, in *Solid State Physics,* edited by F. Seitz and D. Turnbull (Academic, New York, 1955), Vol. 1, p. 193; L. Guttman, *Order-Disorder Phenomena in Metals,* in *Solid State Physics,* edited by F. Seitz and D. Turnbull (Academic, New York, 1956), Vol. 3, p. 145.

[2]M. Hansen, *Constitution of Binary Alloys* (McGraw-Hill, New York, 1958), p. 198; R. P. Elliott, *Constitution of Binary Alloys, First Supplement* (McGraw-Hill, New York, 1965), p. 87; F. A. Shunk, *Constitution of Binary Alloys, Second Supplement* (McGraw-Hill, New York, 1969), p. 68.

[3]T. Hashimoto, K. Nishimura, and Y. Takeuchi, J. Phys. Soc. Jpn. 45, 1127 (1978).

[4]N. R. Lokhande and C. Mande, Phys. Status Solidi B 102, K11 (1980).

[5]T. M. Hayes and J. B. Boyce, in *Solid State Physics,* edited by H. Ehrenreich, F. Seitz, and D. Turnbull (Academic, New York, 1982), Vol. 37, p. 173.

[6]B.-K. Teo and P. A. Lee, J. Am. Chem. Soc. 101, 2815 (1979).

[7]J. M. Cowley, J. Appl. Phys. 21, 24 (1950).

[8]J. M. Cowley, Phys. Rev. 77, 669 (1950).

[9]H. Bethe, Proc. R. Soc. London Ser. A 150, 552 (1935).

[10]Z. W. Wilchinsky, J. Appl. Phys. 15, 806 (1944).

[11]S. C. Moss, J. Appl. Phys. 35, 3547 (1964).

[12]N. S. Golosov, L. E. Popov, and L. Ya. Pudan, J. Phys. Chem. Solids 34, 1157 (1973).

[13]R. C. Kittler and L. M. Falicov, Phys. Rev. B 19, 291 (1979).

[14]R. Kikuchi, Phys. Rev. 81, 988 (1951).

[15]H. L. Yakel, J. Appl. Phys. 33, 2439 (1962).

[16]E. Sevillano, H. Meuth, and J. J. Rehr, Phys. Rev. B 20, 4908 (1979).

[17]S. Siegel, Phys. Rev. 57, 537 (1940).

[18]G. C. Kuczynski, M. Doyama, and M. E. Fine, J. Appl. Phys. 27, 651 (1956).